FI SEVIER

Contents lists available at ScienceDirect

Free Radical Biology and Medicine

journal homepage: www.elsevier.com/locate/freeradbiomed



Original Contribution

Neuroprotective effects of the mitochondria-targeted antioxidant MitoQ in a model of inherited amyotrophic lateral sclerosis



Ernesto Miquel^a, Adriana Cassina^{b,c}, Laura Martínez-Palma^a, José M. Souza^{b,c}, Carmen Bolatto^a, Sebastián Rodríguez-Bottero^a, Angela Logan^d, Robin A.J. Smith^e, Michael P. Murphy^d, Luis Barbeito^f, Rafael Radi^{b,c}, Patricia Cassina^{a,c,*}

- a Departamento de Histología y Embriología, Facultad de Medicina, Universidad de la República, 11800 Montevideo, Uruguay
- ^b Departamento de Bioquímica, Facultad de Medicina, Universidad de la República, 11800 Montevideo, Uruguay
- ^c Center for Free Radical and Biomedical Research, Facultad de Medicina, Universidad de la República, 11800 Montevideo, Uruguay
- ^d Mitochondrial Biology Unit, Medical Research Council, Cambridge CB2 0XY, UK
- ^e Department of Chemistry, University of Otago, Dunedin 9054, New Zealand
- f Institut Pasteur de Montevideo, 11400 Montevideo, Uruguay

ARTICLE INFO

Article history: Received 19 November 2013 Received in revised form 10 February 2014 Accepted 17 February 2014 Available online 26 February 2014

Keywords: Amyotrophic lateral sclerosis Free radicals Nitroxidative stress Antioxidants Mitochondria MitoQ

ABSTRACT

Amyotrophic lateral sclerosis (ALS) is a fatal neurodegenerative disorder characterized by motor neuron degeneration that ultimately results in progressive paralysis and death. Growing evidence indicates that mitochondrial dysfunction and oxidative stress contribute to motor neuron degeneration in ALS. To further explore the hypothesis that mitochondrial dysfunction and nitroxidative stress contribute to disease pathogenesis at the in vivo level, we assessed whether the mitochondria-targeted antioxidant [10-(4, 5-dimethoxy-2-methyl-3,6-dioxo-1,4-cyclohexadien-1-yl)decyl]triphenylphosphonium methane sulfonate (MitoQ) can modify disease progression in the SOD1^{G93A} mouse model of ALS. To do this, we administered MitoQ (500 µM) in the drinking water of SOD1^{G93A} mice from a time when early symptoms of neurodegeneration become evident at 90 days of age until death. This regime is a clinically plausible scenario and could be more easily translated to patients as this corresponds to initiating treatment of patients after they are first diagnosed with ALS. MitoQ was detected in all tested tissues by liquid chromatography/mass spectrometry after 20 days of administration. MitoQ treatment slowed the decline of mitochondrial function, in both the spinal cord and the quadriceps muscle, as measured by high-resolution respirometry. Importantly, nitroxidative markers and pathological signs in the spinal cord of MitoQ-treated animals were markedly reduced and neuromuscular junctions were recovered associated with a significant increase in hindlimb strength. Finally, MitoQ treatment significantly prolonged the life span of SOD1^{G93A} mice. Our results support a role for mitochondrial nitroxidative damage and dysfunction in the pathogenesis of ALS and suggest that mitochondria-targeted antioxidants may be of pharmacological use for ALS treatment.

© 2014 Elsevier Inc. All rights reserved.

E-mail address: pcassina@fmed.edu.uy (P. Cassina).

ALS¹ is a fatal and devastating neurodegenerative disease that affects motor neurons, with no effective therapy available, leading to death within 3–5 years of diagnosis [1]. Mitochondrial dysfunction and oxidative stress in both the neurons and the surrounding glia have been implicated as a key part of the pathogenic process [2]. Reactive oxygen and nitrogen species are required for the execution of motor neuron apoptosis under various experimental conditions [3–5]. In addition, reactive astrocytes represent another source of nitric oxide and oxidants that in turn contributes to motor neuron apoptosis [5–7], suggesting that oxidative stress is involved in astrocyte-mediated motor neuron loss. As mitochondria are both the main producers and the targets of reactive species, targeting mitochondrial oxidative damage may be clinically useful in ALS.

Many antioxidant approaches have shown beneficial effects on animal models of ALS but have not been effective in human ALS

Abbreviations: ALS, amyotrophic lateral sclerosis; SOD1 G93A , ALS-linked superoxide dismutase 1 bearing the G93A mutation; MitoQ, [10-(4,5-dimethoxy-2-methyl-3,6-dioxo-1,4-cyclohexadien-1-yl)decyl]triphenylphosphonium; TPP, triphenylphosphonium; decylTPP, decyltriphenylphosphonium cation; LC/ESI-MS/MS, liquid chromatography/electrospray ionization-mass spectrometry; MRM, multiple-reaction monitoring; d15-MitoQ, deuterated MitoQ; IS, internal standard; FCCP, carbonyl cyanide p-trifluoromethoxyphenylhydrazone; UCR, uncoupling control ratio; TBS, Tris-buffered saline; PBS, phosphate-buffered saline; BSA, bovine serum albumin; GFAP, glial fibrillary acidic protein; HO-1, heme oxygenase-1; HNE, 4-hydroxynonenal-protein adduct; EDL, extensor digitorum longus muscle; TMR-BgTx, tetramethylrhodamine-conjugated α -bungarotoxin; non-Tg, nontransgenic; ARE, antioxidant-response element; RONS, reactive oxygen and nitrogen species

^{*} Corresponding author at: Universidad de la República, Departamento de Histología y Embriología, Facultad de Medicina, Av. General Flores 2125, Montevideo 11800, Uruguay.

patients [8]. In particular, two molecules that stimulate mitochondrial function and prolonged survival in ALS mice, coenzyme Q10 and creatine, have been tested in phase II clinical trials and failed to demonstrate efficacy against disease progression [9,10]. These two studies, despite measuring elevated plasma levels of the compounds and assessing their ability to cross the blood-brain barrier, did not address the elevated free radical production and oxidative damage at the mitochondrial level. This is relevant because mitochondria constitute a main source of free radical production. An emerging pharmacological approach to treating mitochondrial disorders is to use mitochondria-targeted antioxidants that concentrate specifically within mitochondria in vivo to selectively decrease mitochondrial oxidative damage [11–13]. The most widely used mitochondria-targeted antioxidant to date is MitoQ, which comprises a triphenylphosphonium (TPP) functionality conjugated to an antioxidant ubiquinone moiety [14]. MitoQ is accumulated within mitochondria in vivo in response to the large mitochondrial membrane potential (negative inside) and there protects mitochondria from oxidative damage. Mitochondria are reported to be a key intracellular site for the generation of reactive species in a wide range of pathologies, and consequently MitoQ has been shown to mitigate oxidative damage in various disease animal models [15], including Alzheimer [16,17] and Parkinson [18] diseases.

The most widely used animal model of ALS is the transgenic mouse expressing a familial ALS-linked SOD1 mutation, which generally develops progressive motor neuron degeneration resembling many aspects of ALS in human patients [19,20]. Studies in SOD1 mutant mice have demonstrated "non-cell autonomous" effects of the mutations, highlighting the important role of glia in motor neuron support [21,22]. Disease onset seems to be dependent on the expression of mutant SOD1 in motor neurons, and the expression of mutant SOD1 in glial cells modulates the rate of degeneration. Interestingly, the toxicity of mutant SOD1 in cultured motor neurons [23] and astrocytes [24] was prevented by their treatment with low concentrations (nM) of MitoQ. Together, these results suggest that MitoQ is a promising candidate for ALS treatment. To further support this hypothesis we tested its ability to affect disease progression in the SOD1^{G93A} mouse model of ALS. To do this we administered MitoQ orally to ALS mice, starting at 90 days of age, when symptoms are already evident [25]. This regime mimics the clinical situation more closely, as this corresponds to initiation of therapy after first diagnosis and would indicate if this therapy may be translatable to the clinic. We then analyzed the effects of MitoQ on nitroxidative stress markers and key features of disease progression: survival, motor performance, neuronal loss, astrocytosis, and neuromuscular plaque decline. This approach may represent a novel mitochondria-targeted therapy for ALS.

Materials and methods

Materials

All reagents were obtained from Sigma Chemical Co (St. Louis, MO, USA) unless otherwise specified. MitoQ as MS010 (an \sim 20% w/w mixture of MitoQ and β -cyclodextrin) and decyltriphenylphosphonium bromide (decylTPP) were obtained from Antipodean Pharmaceuticals, Inc. Deuterated MitoQ (d₁₅-MitoQ) was synthesized as described previously [17].

Ethics statement

Procedures using laboratory animals were in accordance with the *International Guiding Principles for Biomedical Research Involving Animals*, as issued by the Council for the International Organizations of Medical Sciences, and were approved by Institutional Animal Committee Resolution No. 66 (Exp. 071140-001465-10), Comisión Honoraria de Experimentación Animal de la Universidad de la República (http://www.chea.udelar.edu.uy).

Animals

Transgenic ALS mice carrying the G93A mutated human SOD1, strain B6SJL-TgN(SOD1-G93A)1Gur [19], were obtained from The Jackson Laboratory (Bar Harbor, ME, USA). The strain was maintained by breeding hemizygous male carriers to B6SJLF1 female hybrids. The offspring were genotyped as previously described [24]. Transgenic mice hemizygous for the SOD1 G93A transgene and non-Tg littermates were used for analysis. The mice were housed under controlled conditions with free access to food and drinking water.

MitoQ treatment trial

Male and female transgenic mice and nontransgenic littermates were divided randomly into the following groups: (A) transgenic and nontransgenic mice that received MitoQ, (B) transgenic and nontransgenic mice that received equal concentrations of decyITPP bromide to determine if the TPP cation had any nonspecific effects, and (C) transgenic and nontransgenic control groups that received regular drinking water. MitoQ and decylTPP were administered as β-cyclodextrin complexes (Antipodean Pharmaceuticals) [26] at a 500 µM concentration of MitoQ or decylTPP in the drinking water supplied ad libitum, with fresh solutions made twice a week. In a previous study, this concentration yielded a daily dose of 3.2 µmol MitoQ/day/mouse or 95-138 µmol MitoQ/day/kg, showed no toxicity, and had no significant effect on animal body weight or food and liquid consumption [27]. Treatment was administered from 90 days of age (early symptomatic stage [19]) until death. Animals were observed weekly for onset of disease symptoms, as well as progression to death. Disease onset was scored as the first observation of abnormal gait or overt hindlimb weakness. End stage of the disease was scored as complete paralysis of both hindlimbs and the inability of the animal to right itself within 20 s of being placed on its side. When this condition was met, the mice were euthanized to limit animal suffering.

Grip strength measurements

Motor function was tested with a grip strength meter (San Diego Instruments, San Diego, CA, USA). Tests were performed by allowing the animal to grasp the platform with both hindlimbs, followed by pulling the animal until it released the platform. The force measurement was recorded twice a week from week 6 (baseline) until death in five separate trials.

Quantification of tissue MitoQ content

Groups of mice were treated as detailed above for 20 days and brain, heart, liver, and quadriceps muscle samples were dissected, weighed, snap-frozen, and stored at $-80\,^{\circ}$ C. Protein concentrations were measured in tissue homogenates by Bradford assay, using BSA as protein standard. Quantification of MitoQ was performed by liquid chromatography coupled to electrospray ionization/mass spectrometry on an ion trap mass spectrometer (Qtrap2000; Applied Biosystems-MDS Sciex) [28]. Electrospray ionization of MitoQ in positive mode generated a m/z signal of 583.5 and this ion was fragmented to obtain a m/z 441.3, so using multiple-reaction monitoring (MRM) mode a quantification protocol can be set following the transition 583.5/441.3 and 598.3/456.3 for d_{15} -MitoQ simultaneously [29]. MitoQ was measured

relative to a deuterated IS; 20 (for brain) and 5 pmol (for other tissues) of d_{15} -MitoQ was added to the tissue homogenate before the organic extraction. The organic extraction of MitoQ was performed as described [27]. Standard curves of tissue homogenates spiked with MitoQ and IS were linear from 0 to 100 pmol MitoQ/100 mg tissue protein, and the assay could detect 0.1 pmol MitoQ/100 mg protein.

Mitochondrial respiration studies

Oxygen consumption studies to evaluate mitochondrial respiratory activity were performed on spinal cord and muscle tissue using an Oxygraph 2K (Oroboros Instruments Corp.) as described previously [30], with minor modifications. Briefly, 90-day-old mice were treated with MitoQ or vehicle for 20 days (n = 3 per group) and immediately after sacrifice lumbar spinal cords and quadriceps muscles were dissected. Tissue samples of 7-10 mg were immediately rinsed in respiration medium (sucrose 110 mM, Mops 60 mM, EGTA 0.5 mM, BSA 1 g/L, MgCl₂ 3 mM, KH₂PO₄ 10 mM, Hepes 20 mM, pH 7.1) and introduced into the Oroboros Oxygraph 2K chamber for high-resolution respirometry at 37 °C. After basal respiration was recorded, glutamate (10 mM)/malate (2 mM), succinate (10 mM), and ADP (1-5 mM) were added to ensure maximal availability of respiratory precursors (as the tissue typically exhibits enhanced membrane permeability due to the mechanical extraction procedures). Then, $2\,\mu\text{g}/\text{ml}$ oligomycin (ATPase inhibitor) was added followed by successive boluses of 0.5 µM FCCP (carbonyl cyanide p-trifluoromethoxyphenylhydrazone) until reaching the maximum rate of oxygen consumption. Finally, 2.5 μM antimycin A (complex III inhibitor) was added as described [31]. The use of antimycin A assists in discriminating mitochondrial from residual (non-electron transport chain-dependent) oxygen consumption. Uncoupling control ratio (UCR) was calculated as UCR = (maximum uncoupled flux (FCCP) – antimycin A-inhibited flux)/(routine respiration – antimycin A-inhibited flux) of tissue respiring. The rate of oxygen consumption was calculated by means of the equipment software (DatLab) and expressed as O_2 flux per mass (pmol s⁻¹ mg⁻¹). Routine (basal) respiration reflects the state of activation of the tissue according to the ATP demand. It is usually controlled strongly by ATP turnover and partly by substrate oxidation and proton leak. UCR is an expression of excess capacity of the electron transport system relative to routine (basal) respiration.

Immunoblot analysis

Mice were treated with MitoQ as described above. After 20 days of treatment, the mice were sacrificed, their brains were dissected, and crude mitochondrial preparations were obtained by differential centrifugation. Briefly, one brain hemisphere was removed, washed extensively, minced, and homogenized with a small tissue grinder. Tissue fragments were disrupted using a Potter-Elvehjem homogenizer in homogenization buffer (110 mM sucrose, 60 mM morpholinepropanesulfonic acid, 0.5 mM EGTA, 1 g/L BSA, 3 mM MgCl₂, 10 mM KH₂PO₄, 20 mM Hepes, pH 7.1) and centrifuged 10 min at 1500 g, and mitochondria were isolated from the supernatant by centrifugation at 15,000 g for 10 min. Mitochondrial pellets were resuspended in a minimal volume of homogenization buffer. Mitochondrial proteins (50 µg) were resolved by electrophoresis on 12% SDS-polyacrylamide gels and transferred to polyvinylidene difluoride membranes (Thermo). The membranes were blocked for 1 h in TBS-T (Tris-buffered saline with 0.6% Tween 20) plus 5% BSA and probed for 60 min at room temperature with a rabbit polyclonal anti-3-nitrotyrosine antibody at a 1:1000 dilution [32] in BSA-TBS-T. After a wash in TBS-T, horseradish peroxidaseconjugated anti-rabbit secondary antibody (1:2500) was applied for 60 min at room temperature. Proteins were visualized with ECL Western blotting substrate (Pierce Biotechnology). β -Actin was used as a loading control. Densitometric analysis was performed using Image] software.

Histological analysis and immunofluorescence

Transgenic and nontransgenic mice (n = 3 per group) treated as described above for 20 days were transcardially perfused with 4% paraformaldehyde fixative in PBS under deep anesthesia (pentobarbital, 50 mg/kg ip). The spinal cords were postfixed and embedded in Paraplast and 5-µm-thick sections were obtained. Staining with toluidine blue was performed for motor neuron counting. For immunofluorescence studies, heating antigen retrieval with citrate buffer was performed in a microwave oven and endogen peroxidase was blocked with 3% hydrogen peroxide diluted in methanol when necessary. After permeabilization (0.2% Triton X-100 in PBS) and blocking of nonspecific antibody binding (2% BSA, 0.2% Triton X-100 in PBS), sections were incubated with the following primary antibodies: mouse monoclonal Cy-3-conjugated anti-glial fibrillary acidic protein (GFAP, 1:600, overnight; Sigma), rabbit polyclonal anti-heme oxygenase-1 (HO-1, 1:400, overnight; Stressgen, Enzo Life Sciences), rabbit anti-3nitrotyrosine (1:50, 72 h [32]) or goat anti-4-hydroxynonenal protein adducts (HNE, 1:100, 72 h; Abcam). GFAP-labeled sections were washed and mounted with glycerol. For HO-1 detection, a secondary AlexaFluor⁴⁸⁸-conjugated goat anti-rabbit antibody (1:1000; Molecular Probes, Life Technologies) was used. For 3-nitrotyrosine and HNE detection, goat anti-rabbit or donkey anti-goat peroxidase-linked secondary antibodies were applied for 1 h, and the enzymatic activity was detected using an AlexaFluor⁴⁸⁸ tyramide signal amplification system (TSA kit; Molecular Probes). Sections in which primary antibody was omitted were included as negative controls. Images were captured by a Nikon digital camera coupled to a Nikon Eclipse TE 200 epifluorescence microscope.

Evaluation of motor neuron number, astrogliosis, and nitroxidative stress markers in the spinal cord

The number of motor neurons was quantified by counting every cell on lamina IX of Rexed displaying motor neuron morphology with nucleus and nucleolus on every fifth toluidine-blue-stained 5-µm section (at least 25 sections per animal) through the lumbar spinal cord. ImageJ software (NIH) tools were used for astrogliosis and nitroxidative marker quantification. Astrogliosis was evaluated on images obtained from every fifth GFAP-immunostained section (20 sections from each group). Ventral horn area occupied by GFAP immunofluorescence was measured and expressed as a percentage of total ventral horn area in each section. Nitrotyrosine and HNE immunoreactivity in the spinal cord ventral horn were quantified by measuring mean gray value in at least 20 images from nonconsecutive sections per group. Mean gray value measured in images from negative control sections was subtracted from raw data. HO-1immunoreactive glial-like cells were counted in the ventral horn from at least 10 sections per animal with the aid of a Cell Counter plug-in and expressed as the number of immunoreactive cells per area.

Neuromuscular junction measurements

The extensor digitorum longus (EDL) and the soleus muscles from the same animals used for oxygen consumption studies were dissected immediately after sacrifice. Muscles were immersed for 60 min in 0.5% paraformaldehyde in PBS, rinsed with PBS, and mechanically dissociated into small bundles of fibers. The teased fibers were incubated with a blocking buffer (50 mM glycine, 1% BSA, and 0.5% Triton X-100) for 3 h and then in tetramethylrhodamine-conjugated α -bungarotoxin (TMR-BgTx; 1:1500; Sigma) overnight at

4 °C. Fibers were washed in PBS and left overnight at 4 °C in glycerol—Tris, pH 8.8 (4:1), which was used as mounting medium for all the preparations. Images were acquired using an Olympus IX81 epifluor-escence microscope. For each muscle the images of 15–35 neuro-muscular junctions were taken and analyzed using Adobe Photoshop software. The total area, defined as the area delimited by the external outline of the TMR-BgTx-stained endplate marked with the Lasso tool, including both stained and unstained areas, was measured. The resulting numbers of selected pixels were counted with the Histogram tool. Data are expressed as a percentage of the neuromuscular junction total area from nontransgenic control animals.

Statistics

Survival curves were compared by Kaplan–Meier analysis with the log-rank test using SigmaPlot 12 (Systat Software). Quantitative data were expressed as the mean \pm SEM and Student's t test or ANOVA followed by the Student–Newman–Keuls test was used for statistical analysis, with p < 0.05 considered significant. When the normality test failed, comparison of the means was performed by one-way ANOVA on ranks followed by the Kruskal–Wallis test. All statistics computations were performed using SigmaPlot 12 (Systat Software) or GraphPad Prism 5 (GraphPad Software).

Results

Orally administered MitoQ accumulated within mice tissues

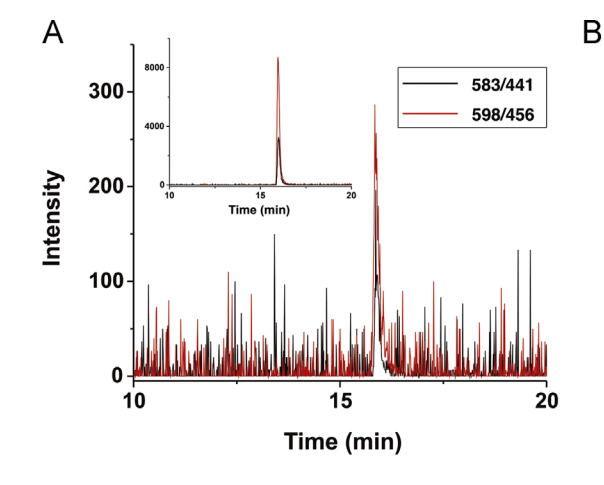
To evaluate the availability of MitoQ within tissues of orally treated mice, SOD1 G93A mice and non-Tg littermates were administered 500 μ M MitoQ in their drinking water from early onset of symptoms (90 days of age) for 20 days. After sacrifice, tissue samples were obtained and analyzed by LC/ESI–MS/MS. We were able to detect MitoQ in brain, liver, heart, and muscle from the treated animals (Fig. 1). Typical LC/MRM chromatograms for MitoQ and d15-MitoQ standards are shown in Fig. 1A (inset). Extracted MitoQ and d15-MitoQ from the heart of a MitoQ-treated mouse are shown in Fig. 1A. The steady-state accumulation of MitoQ for various tissues is shown in Fig. 1B. Therefore, long-term administration of MitoQ in the drinking water led to the substantial steady-state accumulation of MitoQ within mouse brain, liver, heart, and muscle in our experiments.

MitoQ administration slowed the mitochondrial function decline in lumbar spinal cord and muscle

To assess whether oral administration of MitoQ was affecting mitochondrial function in target tissues we performed highresolution respirometry in spinal cord and quadriceps muscle tissue obtained from non-Tg and SOD1^{G93A} mice after 20 days of MitoQ or decylTPP treatment (from 90 days of age, at the beginning of symptoms). High-resolution respirometry in lumbar spinal cord and muscle tissue was monitored and the UCR was calculated. Nontransgenic animal tissues exhibited a basal respiratory rate of around 6-7 and 7-8 pmol O₂ s⁻¹ mg⁻¹ for spinal cord and muscle, respectively; under maximal uncoupling conditions (FCCP) oxygen consumption increased threefold, a value that was decreased to 30% of basal with the addition of antimycin A. In SOD1^{G93A} animals, basal respiratory rates were usually about 60% of nontransgenic animals. The average calculated UCR for spinal cord and quadriceps muscle of nontransgenic animals was 2.6 and 3.8, respectively, and was significantly decreased in the SOD1 G93A mice as shown in Fig. 2. MitoQ-treated SOD1^{G93A} mice exhibited an increase in spinal cord and quadriceps UCR relative to decylTPP-treated or control SOD1^{G93A} mice, to a level similar to that shown for non-Tg mice (Fig. 2). MitoQ administration to non-Tg animals did not significantly affect UCR in either tissue. The mitochondrial function improvement was detected in both males and females without significant differences, so data from both genders were pooled.

MitoQ administration decreased nitroxidative damage in the nervous system

Widespread oxidative damage to proteins, DNA, and lipids is described in ALS and supported by the finding of nitroxidative markers such as 3-nitrotyrosine, malondialdehyde, HNE, oxidized proteins, oxidized DNA, and membrane phospholipid peroxidation (reviewed in [33]). To find out whether MitoQ administration reduced nitroxidative damage we analyzed nitroxidative markers in the brain and the spinal cord of SOD1^{G93A} mice after 20 days of treatment. MitoQ administration mitigated the previously described increase in 3-nitrotyrosine labeling in the nervous system of SOD1^{G93A} mice, in both isolated brain mitochondria (Fig. 3A) and spinal cord ventral horn (Fig. 3B). In addition, we analyzed HNE immunoreactivity as a lipid peroxidation marker and found reduced



Tissue	pmoles MitoQ/ 100 mg protein
SOD1 ^{G93A} MitoQ	
Brain	3.9
Quadriceps	12.0
Heart	19.2
Liver	15.1
SOD1 ^{G93A} Control	
Brain	0
Quadriceps	0
Non Tg MitoQ	
Brain	4.2
Quadriceps	10.7
Non Tg Control	
Brain	0
Quadriceps	0

Fig. 1. MitoQ detection in brain, muscle, heart, and liver from orally treated mice. (A) Multiple-reaction monitoring of MitoQ (black line) and d_{15} -MitoQ (red line) following 583/441 and 598/456 transitions, respectively. The graph shows a representative record from a heart sample of a MitoQ-treated SOD1^{G93A} mouse. The inset shows the separation and detection of MitoQ and d_{15} -MitoQ standards by HPLC/MS. (B) Summary of the quantification of MitoQ in the indicated tissues in terms of picomoles of MitoQ per 100 mg of proteins. (For interpretation of the references to color in this figure legend, the reader is referred to the web version of this article.)

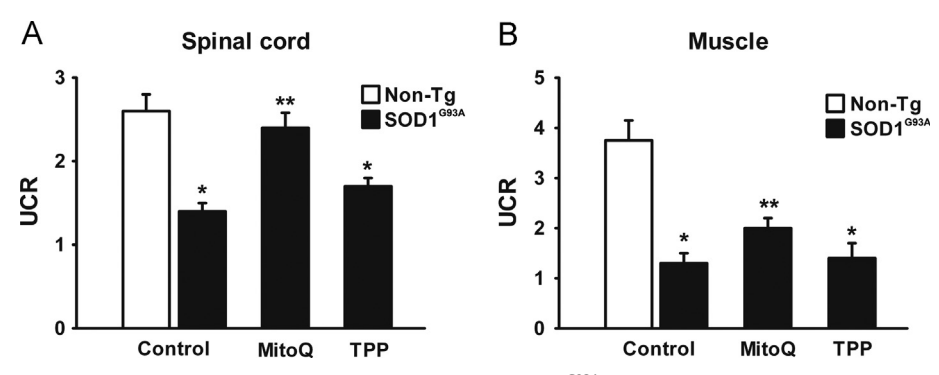


Fig. 2. MitoQ improved mitochondrial respiratory function in spinal cord and muscle from SOD1^{G93A} mice. Uncoupling control ratio (UCR) is shown for (A) spinal cord and (B) quadriceps muscle mitochondria from non-Tg or SOD1^{G93A} mice treated with MitoQ or decylTPP (TPP) as indicated. Data are expressed as the mean \pm SEM from three independent experiments. *p < 0.05, significantly different from non-Tg control. **p < 0.05, significantly different from SOD1^{G93A} control.

labeling in the spinal cord of MitoQ-treated compared to control SOD1^{G93A} mice (Fig. 3C). In spinal cord slices from non-Tg animals, both 3-nitrotyrosine and HNE immunolabeling was very low, similar to that found in SOD1^{G93A} spinal cord slices in which primary antibodies were omitted (negative controls, data not shown). As further proof that MitoQ reduced nitroxidative stress in this model, we studied the expression of an antioxidant-response element (ARE)-containing gene, HO-1, which has been described to be upregulated in glial cells in SOD1^{G93A} rats [34]. We found that the number of glial-like HO-1-immunoreactive cells per area in the spinal cord of SOD1^{G93A} mice was significantly reduced by MitoQ treatment (Fig. 3D). As previously described for SOD1^{G93A} rats [34], some HO-1 immunoreactivity was found in neurons but not in glial-like cells in non-Tg mouse spinal cord (data not shown).

MitoQ administration reduced motor neuron loss and astrogliosis in the lumbar spinal cord

To further characterize the effects of MitoQ on SOD1^{G93A} mice, another group of animals was sacrificed after 20 days of treatment to study the motor neuron population and GFAP immunoreactivity in the spinal cord as indicators of disease progression and astrogliosis, respectively. There was a significant preservation of motor neuron somas in the Rexed lamina IX of the spinal cord ventral horn from MitoQ-treated SOD1^{G93A} mice compared to untreated mice (non-Tg, 16.2 ± 0.5 ; control SOD1^{G93A}, 6.9 ± 0.5 ; MitoQ-treated SOD1^{G93A}, 10.0 ± 0.3 ; Fig. 4A). Accordingly, a marked reduction (54%) in GFAP content was detected in the spinal cord from MitoQ-treated SOD1^{G93A} mice compared with the vehicle-treated group (Fig. 4B).

MitoQ administration preserved neuromuscular junctions

Alterations in neuromuscular junction morphology followed by axonal degeneration have been described as early events in both ALS animal models and patients [35]. To further analyze the effects of MitoQ treatment on SOD1^{G93A} mice, we studied the acetylcholine receptor distribution in the postsynaptic element of the neuromuscular junction in EDL and soleus muscles using fluorescent bungarotoxin. After 20 days of MitoQ treatment, EDL neuromuscular junctions from SOD1^{G93A} animals exhibited an increased postsynaptic area compared to untreated mice (Fig. 5). This effect was not seen in soleus muscles (data not shown).

MitoQ administration increased grip strength and prolonged survival of $SOD1^{G93A}$ mice

The MitoQ beneficial effects detected on SOD1^{G93A} mouse mitochondrial function and spinal cord pathology prompted us

to test the effects of MitoQ on motor symptoms and life span of the animals. Chronic oral MitoQ administration to SOD1 $^{\rm G93A}$ mice significantly increased the mean survival in both males and females (males, control 124.0 \pm 1.7 days, MitoQ 130.1 \pm 2.0 days; females, control 127.6 \pm 1.9 days, MitoQ 134.8 \pm 2.7 days; Fig. 6A) as indicated by Kaplan–Meier survival analysis. Data from the decylTPP-treated group exhibited a large variability and were not statistically different from neither the MitoQ nor the control group (data not shown). Regarding the effects of MitoQ on motor performance of SOD1 $^{\rm G93A}$ mice, it is interesting to note that MitoQ administration significantly improved grip-strength performance at the end stage of the disease (Fig. 6B), although this effect could be detected only in female mice.

Discussion

Our results show that oral administration of the mitochondriatargeted antioxidant MitoQ to SOD1^{G93A} mice starting at the onset of the symptoms had a pharmacological effect extending survival and improving grip strength. This improved animal behavior was associated with a slower decline in mitochondrial respiratory activity in the spinal cord and muscle; reduction in nitroxidative stress markers, astrogliosis, and motor neuron loss in the spinal cord; and preservation of neuromuscular junctions.

Oxidative stress and mitochondrial alterations have long been associated with ALS. As a result, various antioxidant treatments have been assayed in the ALS animal models and found to be beneficial, as they slowed disease progression, including nitrones such as DMPO [36], nitroxides such as Tempol [37], and SOD1 mimetics [38,39]. Mitochondria are the main source of cellular reactive oxygen and nitrogen species (RONS), whose production further increases if mitochondria are damaged [40,41]. On the other hand, mitochondria themselves are a target of RONS, which can impair mitochondrial function [42]. In this context, the development of antioxidants that selectively concentrate in mitochondria provides an opportunity to decipher the impact of mitochondria-generated RONS in the pathogenesis and progression of ALS. The contribution of RONS-caused mitochondrial dysfunction to the neurodegenerative process may depend on the cell type involved [43]. We have previously shown that MitoQ prevented the increased susceptibility to trophic factor deprivation exhibited by motor neurons expressing SOD1^{G93A} compared to non-Tg motor neurons [23]. We also provided evidence that MitoQ treatment of SOD1^{G93A}-expressing astrocytes reduced nitroxidative stress and mitochondrial dysfunction exhibited by these cells and, importantly, reduced their toxicity to motor neurons in cocultures [24]. These results were consistent with the now wellaccepted proposal that mutant SOD1-mediated toxicity within

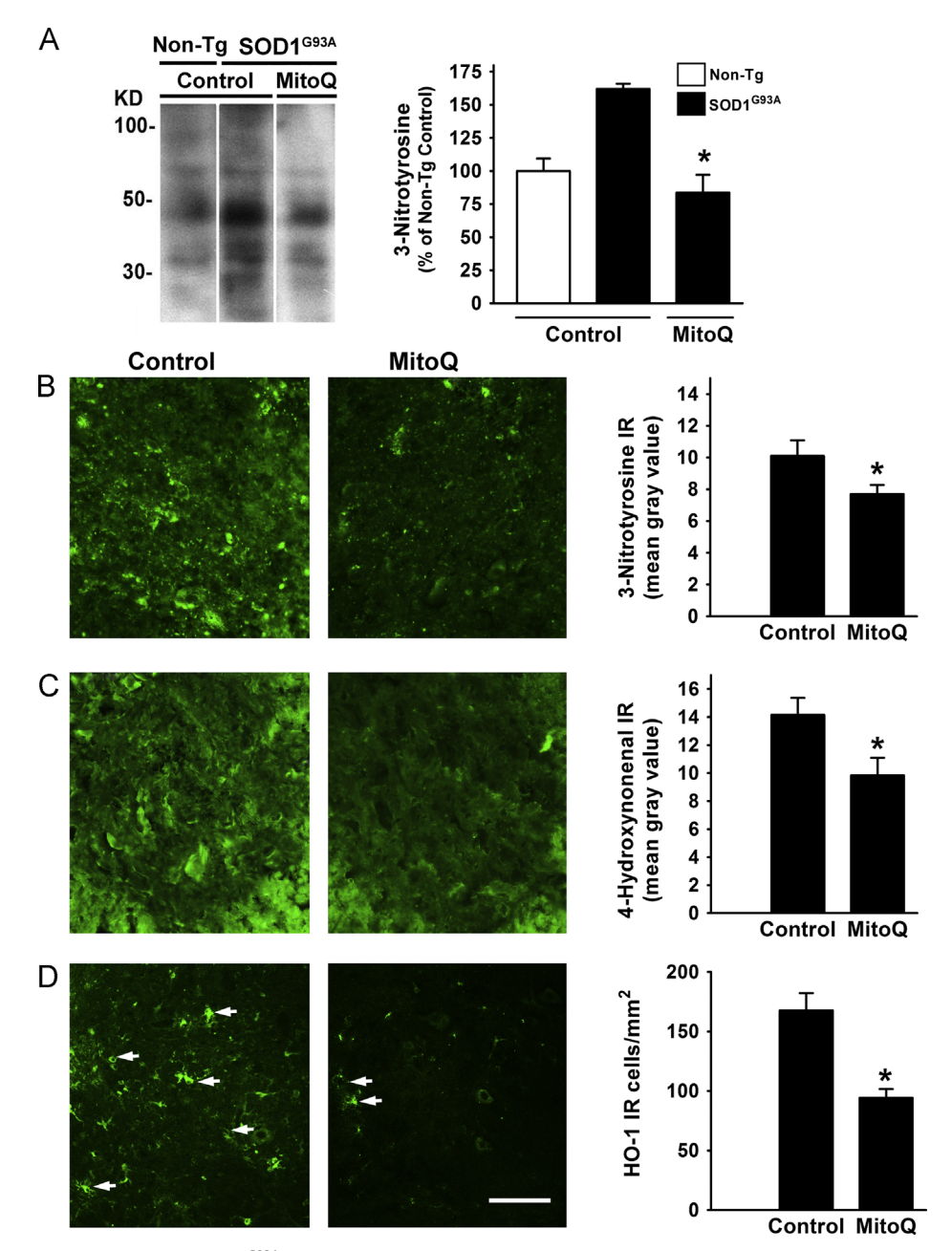


Fig. 3. MitoQ decreased nitroxidative markers in SOD1^{G93A} mouse central nervous system. (A) Representative 3-nitrotyrosine immunoblot of brain mitochondrial proteins from the indicated groups of mice. The graph on the right indicates relative densitometric levels of 3-nitrotyrosine expressed as a percentage of non-Tg control. Data are expressed as the mean \pm SEM from two blots assayed in duplicate. (B, C) Representative images and mean gray value quantification of immunofluorescence for (B) 3-nitrotyrosine and (C) 4-hydroxynonenal-protein adducts in the ventral horn of spinal cord sections from the indicated groups of animals. (D) Representative heme oxygenase-1 immunoreactivity in the same region described for (B) and (C). Note the glial-like immunoreactive cells (arrows). The graph on the right shows the quantification of the number of glial-like immunoreactive cells per area in the ventral horn of the spinal cord of the indicated groups of animals. Data are expressed as the mean \pm SEM from three independent experiments. *p < 0.05, significantly different from SOD1^{G93A} control. Scale bar: 50 μ m (B, C) and 100 μ m (D).

astrocytes and microglia is a central component of the mechanism of disease progression [44–46]. To further assess that hypothesis, in this work we analyzed the effects of chronic MitoQ administration to SOD1^{G93A} mice. Oral administration of MitoQ to ALS mice showed a disease-modifying effect, which further provides a proof of principle that nitroxidative stress at the mitochondrial level plays a significant role in the ALS pathological process. Within mitochondria, the ubiquinone moiety of MitoQ is reduced by complex II to its active ubiquinol form, which protects mitochondria against oxidative damage [14]. Indeed, in the reactions of a variety of oxidants with ubiquinol, the latter is oxidized to ubiquinone, which is readily reduced back to ubiquinol by the respiratory chain [47] and thus it is continually recycled. Therefore,

MitoQ neutralizes a variety of reactive oxygen and nitrogen species and maintains mitochondrial function. This was confirmed in our results by high-resolution respirometry, as the in vivo MitoQ treatment increased the UCR in isolated spinal cord and muscle tissue. We can affirm that this effect was due to the accumulation of ubiquinol within mitochondria instead of the lipophilic cation used to target MitoQ because UCR was reestablished only by MitoQ and not by decylTPP. The MitoQ-dependent ubiquinol cycle in mitochondria could potentially lead to ubisemiquinone radicals promoting increased superoxide radical formation in mitochondria and thus interfere with mitochondrial-derived hydrogen peroxide-dependent cellular signaling; however, the effect of long-term in vivo MitoQ administration on the production of

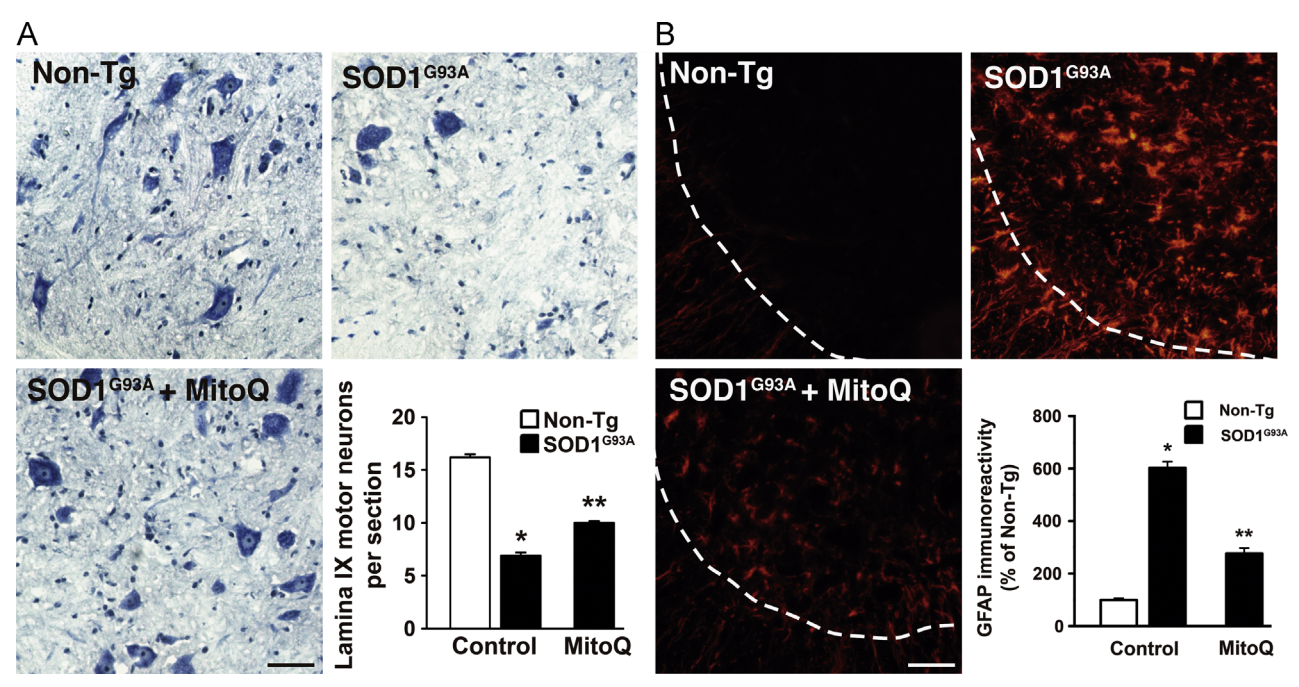


Fig. 4. MitoQ decreased motor neuron loss and astrocyte reactivity in the spinal cord of SOD1^{G93A} mice. (A) Representative Nissl stain in ventral horn spinal cord sections from the indicated groups of mice. The graph indicates the number of neuronal somas located in Rexed lamina IX. (B) Representative GFAP immunofluorescence in ventral horn spinal cord sections from the indicated mice. Dotted lines indicate the limit between gray and white matter. The graph shows the GFAP-immunoreactive area in the ventral horn of the indicated groups of animals as a percentage of non-Tg control. Data are expressed as the mean \pm SEM from at least three animals per group. *p < 0.05, significantly different from non-Tg control; **p < 0.05, significantly different from SOD1^{G93A} control. Scale bar: 50 µm (A) and 100 µm (B).

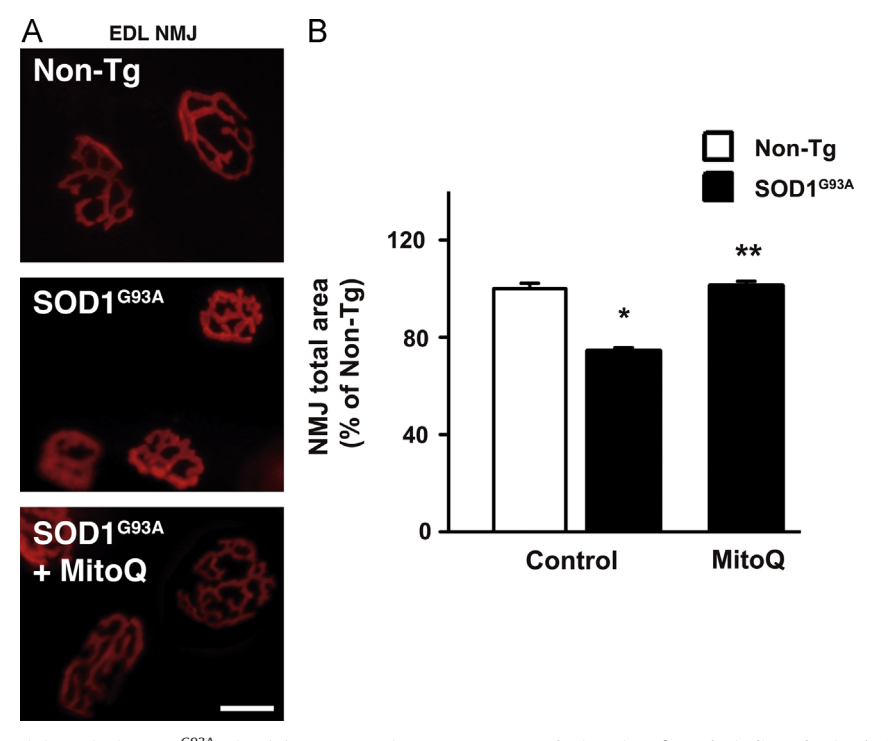
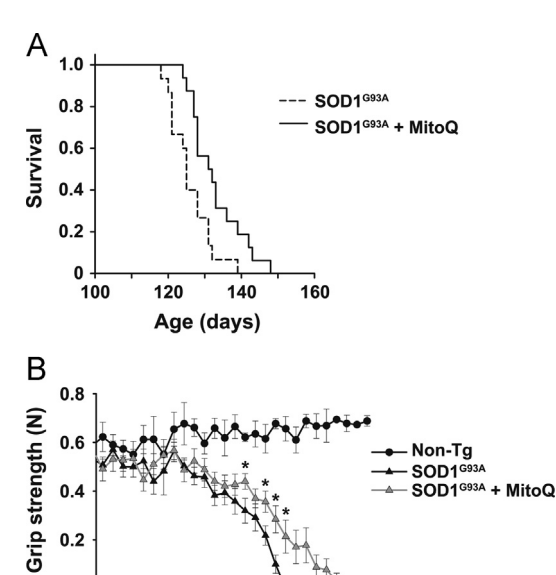


Fig. 5. MitoQ maintained motor unit integrity in SOD1^{G93A} mice. (A) Representative EDL neuromuscular junctions from the indicated animals detected by TMR-BgTx labeling of acetylcholine receptors in the postsynaptic area. (B) Quantification of total TMR-BgTx-stained neuromuscular area in the EDL muscle from the different groups of animals. Data are expressed as a percentage of non-Tg control, mean \pm SEM from 60–100 neuromuscular junctions from two to four animals per group. *p < 0.05, significantly different from non-Tg control; **p < 0.05, significantly different from SOD1^{G93A} control. Scale bar: 50 μ m.

reactive species and redox signaling has been explored in detail [27] and no effects on these processes were found. This is the first report of high-resolution oxymetry in living tissues (in contrast to measurements in isolated mitochondria) directly assessing a beneficial action of mitochondria-targeted antioxidants in respiratory function.

The reduced levels of nitroxidative markers detected in MitoQ-treated mice provide convincing evidence to sustain that the protective mechanisms of MitoQ include attenuation of oxidant formation in vivo as has been reported in other animal models tested [15]. In the present work MitoQ treatment decreased 3-nitrotyrosine levels in isolated brain mitochondria, confirming



0

80

100

Age (days)

Fig. 6. MitoQ increased survival and improved grip strength in orally treated SOD1^{G93A} mice. (A) Kaplan–Meier survival curves from MitoQ-treated and control SOD1^{G93A} mice. MitoQ was administered in drinking water from 90 days of age (symptoms onset) until death. n=15 or 16 animals per group. Data for both genders were pooled as no significant differences were detected among them. p<0.05, Kaplan–Meier log-rank test. (B) Hindlimb grip strength records from non-Tg or SOD1^{G93A} female mice treated with MitoQ or vehicle as indicated. MitoQ-treated non-Tg animals did not show differences from controls and data are not shown in order to simplify the graph. Data are expressed as the mean \pm SEM from 7–10 animals per group. *p<0.05, significantly different from SOD1^{G93A} control.

120

that damage by nitric oxide-derived oxidants is being halted within the organelle. Furthermore, HNE immunoreactivity was also decreased in the MitoQ-treated animals, demonstrating that nitroxidative damage in both proteins and lipids was simultaneously diminished. Indirect support is also provided by the reduced HO-1 immunoreactivity, as increased production of oxidants activates the Nrf2-mediated expression of ARE-containing genes, including HO-1. HO-1 expression is increased in reactive astrocytes in the spinal cord of symptomatic SOD1^{G93A} rats [34]. The finding that MitoQ decreased the number of HO-1-immunoreactive glial-like cells in the $\mathsf{SOD1}^\mathsf{G93A}$ mice spinal cord suggests that reduced RONS-mediated signaling is occurring. In addition, it further supports the contribution of glial cells to ALS pathology. Taken together, our results suggest that reducing nitroxidative damage in mitochondria delays disease progression and pathological signs, offering a therapeutic alternative to include in ALS treatment.

A key requirement for drugs targeting the central nervous system (CNS) is to be able to cross the blood–brain barrier. In this study we were able to detect MitoQ accumulation in brain samples although in lower levels than in other assayed tissues, which probably reflects some limitation of MitoQ to cross the blood–brain barrier. Nonetheless, the levels found in brain were significant and large enough to provide pharmacological effects (*vide infra*). In addition, a recent study using $100~\mu M$ MitoQ in drinking water showed benefits in a transgenic mouse model of Alzheimer disease [16] and also in the MPTP model of Parkinson disease [18], indicating that MitoQ was able to reach the CNS when administrated in a lower dose.

It is interesting to note that MitoQ-treated animals retained increased grip strength until death compared with untreated SOD1^{G93A} animals. Moreover, the EDL muscle fibers of MitoQ-treated mice displayed neuromuscular junctions with preserved size and shape, indicating that MitoQ could delay the progressive neuromuscular junction destruction characteristic of animals with

ALS [48]. The beneficial effects of MitoQ on motor performance were more pronounced in females than in males. However, the improvement in mitochondrial function was detected in both genders. Gender differences have been reported previously in SOD1^{G93A} mutant rats [49] and mice [50–53]. In fact, the SOD1^{G93A} mouse model shows sexual dimorphism, with females living slightly longer [54,55]. In addition, increased susceptibility to oxidative stress of brain cells from male mice compared to female has been demonstrated [56] and particularly increased transgenic SOD1 toxicity on males has also been reported [57]. These differences may explain the gender-dependent differential reaction to MitoQ treatment in grip strength compared to mitochondrial function.

Most therapeutic approaches reported in this mouse model of ALS to date have involved administration of agents long before onset of symptoms, which cannot currently be accomplished in ALS patients as most cases of the disease are sporadic and, consequently, presymptomatic assessment is not possible. In fact, another antioxidant mitochondrial-targeted strategy used in the same mouse model, the cell-permeative peptide antioxidant SS-31, showed benefits, but the treatment was started at 30 days of age [58]. In the present study, we examined the effects of MitoQ administered at the symptom onset to judge its ability to extend survival and preserve motor function in mice that have already initiated the pathological process. Despite this, the MitoQ treatment delayed most pathological signs, indicating that the disease process can still be slowed, and further supports the potential use of MitoQ as a therapeutic option for ALS.

Conclusions

This study supports the potential use of mitochondria-targeted antioxidants to treat ALS. Because mitochondrial dysfunction is a common feature of multiple neurodegenerative disorders [59], mitochondria-targeted antioxidant therapies could also be beneficial for other neurodegenerative diseases. In fact, MitoQ has been proven neuroprotective in animal models of Parkinson disease [18] and Alzheimer disease [16]. The fact that MitoQ has already been authorized for its use in humans [15] further raises the possibility of using it as a therapy to treat ALS and encourages a swift translation of these findings into clinical studies.

Acknowledgments

This work was supported by grants from the Universidad de la República (CSIC Grupos), Uruguay (to R.R.), and the Agencia Nacional de Investigación e Innovación (ANII), Uruguay (ANII-FCE 2011_1_6260 to J.M.S.); a fellowship from the ANII, Uruguay (to E. M.); the Medical Research Council, United Kingdom (to M.P.M.); and the Foundation for Research Science and Technology, New Zealand, and Antipodean Pharmaceuticals (to R.A.J.S.).

References

- [1] Turner, M. R.; Hardiman, O.; Benatar, M.; Brooks, B. R.; Chio, A.; de Carvalho, M.; Ince, P. G.; Lin, C.; Miller, R. G.; Mitsumoto, H.; Nicholson, G.; Ravits, J.; Shaw, P. J.; Swash, M.; Talbot, K.; Traynor, B. J.; Van den Berg, L. H.; Veldink, J. H.; Vucic, S.; Kiernan, M. C. Controversies and priorities in amyotrophic lateral sclerosis. *Lancet Neurol.* 12:310–322; 2013.
- [2] Kawamata, H.; Manfredi, G. Mitochondrial dysfunction and intracellular calcium dysregulation in ALS. Mech. Ageing Dev. 131:517–526; 2010.
- [3] Estevez, A. G.; Crow, J. P.; Sampson, J. B.; Reiter, C.; Zhuang, Y.; Richardson, G. J.; Tarpey, M. M.; Barbeito, L.; Beckman, J. S. Induction of nitric oxide-dependent apoptosis in motor neurons by zinc-deficient superoxide dismutase. *Science* 286:2498–2500; 1999.
- [4] Raoul, C.; Estevez, A. G.; Nishimune, H.; Cleveland, D. W.; deLapeyriere, O.; Henderson, C. E.; Haase, G.; Pettmann, B. Motoneuron death triggered by a

- specific pathway downstream of Fas: potentiation by ALS-linked SOD1 mutations. *Neuron* **35**:1067–1083; 2002.
- [5] Cassina, P.; Peluffo, H.; Pehar, M.; Martinez-Palma, L.; Ressia, A.; Beckman, J. S.; Estevez, A. G.; Barbeito, L. Peroxynitrite triggers a phenotypic transformation in spinal cord astrocytes that induces motor neuron apoptosis. *J. Neurosci. Res.* 67:21–29; 2002.
- [6] Cassina, P.; Pehar, M.; Vargas, M. R.; Castellanos, R.; Barbeito, A. G.; Estevez, A. G.; Thompson, J. A.; Beckman, J. S.; Barbeito, L. Astrocyte activation by fibroblast growth factor-1 and motor neuron apoptosis: implications for amyotrophic lateral sclerosis. J. Neurochem. 93:38–46; 2005.
- [7] Pehar, M.; Cassina, P.; Vargas, M. R.; Castellanos, R.; Viera, L.; Beckman, J. S.; Estevez, A. G.; Barbeito, L. Astrocytic production of nerve growth factor in motor neuron apoptosis: implications for amyotrophic lateral sclerosis. *J. Neurochem.* 89:464–473; 2004.
- [8] Orrell, R. W.; Lane, R. J.; Ross, M. A systematic review of antioxidant treatment for amyotrophic lateral sclerosis/motor neuron disease. *Amyotrophic Lateral Scler.* 9:195–211; 2008.
- [9] Kaufmann, P.; Thompson, J. L.; Levy, G.; Buchsbaum, R.; Shefner, J.; Krivickas, L. S.; Katz, J.; Rollins, Y.; Barohn, R. J.; Jackson, C. E.; Tiryaki, E.; Lomen-Hoerth, C.; Armon, C.; Tandan, R.; Rudnicki, S. A.; Rezania, K.; Sufit, R.; Pestronk, A.; Novella, S. P.; Heiman-Patterson, T.; Kasarskis, E. J.; Pioro, E. P.; Montes, J.; Arbing, R.; Vecchio, D.; Barsdorf, A.; Mitsumoto, H.; Levin, B. Phase II trial of CoQ10 for ALS finds insufficient evidence to justify phase III. Ann. Neurol. 66:235–244: 2009.
- finds insufficient evidence to justify phase III. *Ann. Neurol.* **66:**235–244; 2009.

 [10] Atassi, N.; Ratai, E. M.; Greenblatt, D. J.; Pulley, D.; Zhao, Y.; Bombardier, J.; Wallace, S.; Eckenrode, J.; Cudkowicz, M.; Dibernardo, A. A phase I, pharmacokinetic, dosage escalation study of creatine monohydrate in subjects with amyotrophic lateral sclerosis. *Amyotrophic Lateral Scler.* **11:**508–513; 2010.
- [11] Smith, R. A. J.; Hartley, R. C.; Cocheme, H. M.; Murphy, M. P. Mitochondrial pharmacology. Trends Pharmacol. Sci. 33:341–352; 2012.
- [12] Smith, R. A. J.; Hartley, R. C.; Murphy, M. P. Mitochondria-targeted small molecule therapeutics and probes. *Antioxid. Redox Signaling* 15:3021–3038; 2011.
- [13] Murphy, M. P.; Smith, R. A. J. Targeting antioxidants to mitochondria by conjugation to lipophilic cations. *Annu. Rev. Pharmacol. Toxicol.* 47:629–656; 2007.
- [14] Kelso, G. F.; Porteous, C. M.; Coulter, C. V.; Hughes, G.; Porteous, W. K.; Ledgerwood, E. C.; Smith, R. A. J.; Murphy, M. P. Selective targeting of a redoxactive ubiquinone to mitochondria within cells: antioxidant and antiapoptotic properties. J. Biol. Chem. 276:4588–4596; 2001.
- [15] Smith, R. A. J.; Murphy, M. P. Animal and human studies with the mitochondria-targeted antioxidant MitoQ. Ann. N. Y. Acad. Sci. 1201:96–103; 2010
- [16] McManus, M. J.; Murphy, M. P.; Franklin, J. L. The mitochondria-targeted antioxidant MitoQ prevents loss of spatial memory retention and early neuropathology in a transgenic mouse model of Alzheimer's disease. *J. Neurosci.* 31:15703–15715; 2011.
- [17] Smith, R. A. J.; Porteous, C. M.; Coulter, C. V.; Murphy, M. P. Selective targeting of an antioxidant to mitochondria. Eur. J. Biochem. 263:709–716; 1999.
- [18] Ghosh, A.; Chandran, K.; Kalivendi, S. V.; Joseph, J.; Antholine, W. E.; Hillard, C. J.; Kanthasamy, A.; Kalyanaraman, B. Neuroprotection by a mitochondria-targeted drug in a Parkinson's disease model. *Free Radic. Biol. Med.* **49:**1674–1684; 2010.
- [19] Gurney, M. E.; Pu, H.; Chiu, A. Y.; Dal Canto, M. C.; Polchow, C. Y.; Alexander, D. D.; Caliendo, J.; Hentati, A.; Kwon, Y. W.; Deng, H. X.; et al. Motor neuron degeneration in mice that express a human Cu,Zn superoxide dismutase mutation. *Science* 264:1772–1775; 1994.
- [20] Howland, D. S.; Liu, J.; She, Y.; Goad, B.; Maragakis, N. J.; Kim, B.; Erickson, J.; Kulik, J.; DeVito, L.; Psaltis, G.; DeGennaro, L. J.; Cleveland, D. W.; Rothstein, J. D. Focal loss of the glutamate transporter EAAT2 in a transgenic rat model of SOD1 mutant-mediated amyotrophic lateral sclerosis (ALS). Proc. Natl. Acad. Sci. USA 99:1604–1609; 2002.
- [21] Clement, A. M.; Nguyen, M. D.; Roberts, E. A.; Garcia, M. L.; Boillee, S.; Rule, M.; McMahon, A. P.; Doucette, W.; Siwek, D.; Ferrante, R. J.; Brown Jr R. H.; Julien, J. P.; Goldstein, L. S.; Cleveland, D. W. Wild-type nonneuronal cells extend survival of SOD1 mutant motor neurons in ALS mice. *Science* 302:113–117; 2003.
- [22] Ilieva, H.; Polymenidou, M.; Cleveland, D. W. Non-cell autonomous toxicity in neurodegenerative disorders: ALS and beyond. J. Cell Biol. 187:761–772; 2009.
- [23] Pehar, M.; Vargas, M. R.; Robinson, K. M.; Cassina, P.; Diaz-Amarilla, P. J.; Hagen, T. M.; Radi, R.; Barbeito, L.; Beckman, J. S. Mitochondrial superoxide production and nuclear factor erythroid 2-related factor 2 activation in p75 neurotrophin receptor-induced motor neuron apoptosis. J. Neurosci. 7777-7785: 2007.
- [24] Cassina, P.; Cassina, A.; Pehar, M.; Castellanos, R.; Gandelman, M.; de Leon, A.; Robinson, K. M.; Mason, R. P.; Beckman, J. S.; Barbeito, L.; Radi, R. Mitochondrial dysfunction in SOD1G93A-bearing astrocytes promotes motor neuron degeneration: prevention by mitochondrial-targeted antioxidants. *J. Neurosci.* 28:4115–4122: 2008.
- [25] Levine, J. B.; Kong, J.; Nadler, M.; Xu, Z. Astrocytes interact intimately with degenerating motor neurons in mouse amyotrophic lateral sclerosis (ALS). *Glia* **28**:215–224; 1999.
- [26] Ross, M. F.; Prime, T. A.; Abakumova, I.; James, A. M.; Porteous, C. M.; Smith, R. A. J.; Murphy, M. P. Rapid and extensive uptake and activation of hydrophobic triphenylphosphonium cations within cells. *Biochem. J.* 411:633–645; 2008.
- [27] Rodriguez-Cuenca, S.; Cocheme, H. M.; Logan, A.; Abakumova, I.; Prime, T. A.; Rose, C.; Vidal-Puig, A.; Smith, A. C.; Rubinsztein, D. C.; Fearnley, I. M.; Jones, B. A.; Pope, S.; Heales, S. J.; Lam, B. Y.; Neogi, S. G.; McFarlane, I.; James, A. M.; Smith, R. A. J.; Murphy, M. P. Consequences of long-term oral

- administration of the mitochondria-targeted antioxidant MitoQ to wild-type mice. Free Radic. Biol. Med. 48:161–172; 2010.
- [28] Li, Y.; Zhang, H.; Fawcett, J. P.; Tucker, I. G. Quantitation and metabolism of mitoquinone, a mitochondria-targeted antioxidant, in rat by liquid chromatography/tandem mass spectrometry. *Rapid Commun. Mass Spectrom.* 21:1958–1964: 2007.
- [29] Li, Y.; Fawcett, J. P.; Zhang, H.; Tucker, I. G. Transport and metabolism of MitoQ10, a mitochondria-targeted antioxidant, in Caco-2 cell monolayers. *J. Pharm. Pharmacol.* 59:503–511; 2007.
- [30] Gnaiger, E. Mitochondrial Pathways and Respiratory Control. Innsbruck: Oroboros MiPNet Publications; 2007.
- [31] Miquel, E.; Cassina, A.; Martinez-Palma, L.; Bolatto, C.; Trias, E.; Gandelman, M.; Radi, R.; Barbeito, L.; Cassina, P. Modulation of astrocytic mitochondrial function by dichloroacetate improves survival and motor performance in inherited amyotrophic lateral sclerosis. *PLoS One* 7:e34776; 2012.
- [32] Brito, C.; Naviliat, M.; Tiscornia, A. C.; Vuillier, F.; Gualco, G.; Dighiero, G.; Radi, R.; Cayota, A. M. Peroxynitrite inhibits T lymphocyte activation and proliferation by promoting impairment of tyrosine phosphorylation and peroxynitrite-driven apoptotic death. J. Immunol. 162:3356–3366; 1999.
- [33] Drechsel, D. A.; Estevez, A. G.; Barbeito, L.; Beckman, J. S. Nitric oxide-mediated oxidative damage and the progressive demise of motor neurons in ALS. *Neurotox. Res.* **22:**251–264; 2012.
- [34] Vargas, M. R.; Pehar, M.; Cassina, P.; Martinez-Palma, L.; Thompson, J. A.; Beckman, J. S.; Barbeito, L. Fibroblast growth factor-1 induces heme oxygenase-1 via nuclear factor erythroid 2-related factor 2 (Nrf2) in spinal cord astrocytes: consequences for motor neuron survival. J. Biol. Chem. 280:25571-25579; 2005.
- [35] Fischer, L. R.; Culver, D. G.; Tennant, P.; Davis, A. A.; Wang, M.; Castellano-Sanchez, A.; Khan, J.; Polak, M. A.; Glass, J. D. Amyotrophic lateral sclerosis is a distal axonopathy: evidence in mice and man. *Exp. Neurol.* 185:232–240; 2004.
- [36] Liu, R.; Li, B.; Flanagan, S. W.; Oberley, L. W.; Gozal, D.; Qiu, M. Increased mitochondrial antioxidative activity or decreased oxygen free radical propagation prevent mutant SOD1-mediated motor neuron cell death and increase amyotrophic lateral sclerosis-like transgenic mouse survival. J. Neurochem. 80:488-500; 2002.
- [37] Linares, E.; Seixas, L. V.; Dos Prazeres, J. N.; Ladd, F. V.; Ladd, A. A.; Coppi, A. A.; Augusto, O. Tempol moderately extends survival in a hSOD1(G93A) ALS rat model by inhibiting neuronal cell loss, oxidative damage and levels of nonnative hSOD1(G93A) forms. PLoS One 8:e55868; 2013.
- [38] Crow, J. P.; Calingasan, N. Y.; Chen, J.; Hill, J. L.; Beal, M. F. Manganese porphyrin given at symptom onset markedly extends survival of ALS mice. *Ann. Neurol.* **58**:258–265; 2005.
- [39] Wu, A. S.; Kiaei, M.; Aguirre, N.; Crow, J. P.; Calingasan, N. Y.; Browne, S. E.; Beal, M. F. Iron porphyrin treatment extends survival in a transgenic animal model of amyotrophic lateral sclerosis. *J. Neurochem.* **85**:142–150; 2003.
- [40] Beal, M. F. Mitochondria take center stage in aging and neurodegeneration. Ann. Neurol. 58:495–505: 2005.
- [41] Radi, R.; Cassina, A.; Hodara, R. Nitric oxide and peroxynitrite interactions with mitochondria. *Biol. Chem.* **383**:401–409; 2002.
- [42] Kowaltowski, A. J.; Vercesi, A. E. Mitochondrial damage induced by conditions of oxidative stress. *Free Radic. Biol. Med.* **26**:463–471; 1999.
- [43] Bolaños, J. P.; Moro, M. A.; Lizasoain, I.; Almeida, A. Mitochondria and reactive oxygen and nitrogen species in neurological disorders and stroke: therapeutic implications. *Adv. Drug Delivery Rev.* **61**:1299–1315; 2009.
- [44] Vargas, M. R.; Pehar, M.; Cassina, P.; Beckman, J. S.; Barbeito, L. Increased glutathione biosynthesis by Nrf2 activation in astrocytes prevents p75NTR-dependent motor neuron apoptosis. *J. Neurochem.* 97:687–696; 2006.
- [45] Nagai, M.; Re, D. B.; Nagata, T.; Chalazonitis, A.; Jessell, T. M.; Wichterle, H.; Przedborski, S. Astrocytes expressing ALS-linked mutated SOD1 release factors selectively toxic to motor neurons. *Nat. Neurosci.* 10:615–622; 2007.
- [46] Di Giorgio, F. P.; Carrasco, M. A.; Siao, M. C.; Maniatis, T.; Eggan, K. Non-cell autonomous effect of glia on motor neurons in an embryonic stem cell-based ALS model. *Nat. Neurosci.* 10:608–614; 2007.
- [47] Cocheme, H. M.; Kelso, G. F.; James, A. M.; Ross, M. F.; Trnka, J.; Mahendiran, T.; Asin-Cayuela, J.; Blaikie, F. H.; Manas, A. R.; Porteous, C. M.; Adlam, V. J.; Smith, R. A. J.; Murphy, M. P. Mitochondrial targeting of quinones: therapeutic implications. *Mitochondrion* 7(Suppl):S94–102; 2007.
- [48] Dupuis, L.; Loeffler, J. P. Neuromuscular junction destruction during amyotrophic lateral sclerosis: insights from transgenic models. *Curr. Opin. Pharmacol.* **9**:341–346; 2009.
- [49] Suzuki, M.; Tork, C.; Shelley, B.; McHugh, J.; Wallace, K.; Klein, S. M.; Lindstrom, M. J.; Svendsen, C. N. Sexual dimorphism in disease onset and progression of a rat model of ALS. Amyotrophic Lateral Scler. 8:20–25; 2007
- [50] Kirkinezos, I. G.; Hernandez, D.; Bradley, W. G.; Moraes, C. T. Regular exercise is beneficial to a mouse model of amyotrophic lateral sclerosis. *Ann. Neurol.* 53:804–807; 2003.
- [51] Cudkowicz, M. E.; Pastusza, K. A.; Sapp, P. C.; Mathews, R. K.; Leahy, J.; Pasinelli, P.; Francis, J. W.; Jiang, D.; Andersen, J. K.; Brown Jr R. H. Survival in transgenic ALS mice does not vary with CNS glutathione peroxidase activity. *Neurology* 59:729–734; 2002.
- [52] Mahoney, D. J.; Rodriguez, C.; Devries, M.; Yasuda, N.; Tarnopolsky, M. A. Effects of high-intensity endurance exercise training in the G93A mouse model of amyotrophic lateral sclerosis. *Muscle Nerve* 29:656–662; 2004.

- [53] Alves, C. J.; de Santana, L. P.; dos Santos, A. J.; de Oliveira, G. P.; Duobles, T.; Scorisa, J. M.; Martins, R. S.; Maximino, J. R.; Chadi, G. Early motor and electrophysiological changes in transgenic mouse model of amyotrophic lateral sclerosis and gender differences on clinical outcome. *Brain Res.* 1394:90–104; 2011.
- [54] Choi, C. I.; Lee, Y. D.; Gwag, B. J.; Cho, S. I.; Kim, S. S.; Suh-Kim, H. Effects of estrogen on lifespan and motor functions in female hSOD1 G93A transgenic mice. J. Neurol. Sci. 268:40–47; 2008.
- [55] Scott, S.; Kranz, J. E.; Cole, J.; Lincecum, J. M.; Thompson, K.; Kelly, N.; Bostrom, A.; Theodoss, J.; Al-Nakhala, B. M.; Vieira, F. G.; Ramasubbu, J.; Heywood, J. A. Design, power, and interpretation of studies in the standard murine model of ALS. Amyotrophic Lateral Scler. 9:4–15; 2008.
- [56] Giordano, G.; Tait, L.; Furlong, C. E.; Cole, T. B.; Kavanagh, T. J.; Costa, L. G. Gender differences in brain susceptibility to oxidative stress are mediated by levels of paraoxonase-2 expression. Free Radic. Biol. Med. 58C;98–108; 2013.
- [57] Li, R.; Strykowski, R.; Meyer, M.; Mulcrone, P.; Krakora, D.; Suzuki, M. Male-specific differences in proliferation, neurogenesis, and sensitivity to oxidative stress in neural progenitor cells derived from a rat model of ALS. PLoS One 7:e48581; 2012.
- [58] Petri, S.; Kiaei, M.; Kipiani, K.; Chen, J.; Calingasan, N. Y.; Crow, J. P.; Beal, M. F. Additive neuroprotective effects of a histone deacetylase inhibitor and a catalytic antioxidant in a transgenic mouse model of amyotrophic lateral sclerosis. *Neurobiol. Dis.* 22:40–49; 2006.
- [59] Schon, E. A.; Przedborski, S. Mitochondria: the next (neurode)generation. Neuron 70:1033-1053; 2011.